ELSEVIER

www.elsevier.nl/locate/jorganchem

Journal of Organometallic Chemistry 604 (2000) 248–259

Journal of Organo metallic Chemistry

Schiff base linked ferrocenyl complexes for second-order nonlinear optics

Sushanta K. Pal, Anu Krishnan, Puspendu K. Das, Ashoka G. Samuelson *

Department of Inorganic and Physical Chemistry, Indian Institute of Science, Bangalore 560 012, India

Received 18 February 2000; received in revised form 26 April 2000

Abstract

A series of substituted ferrocenyl compounds where one of the cyclopentadienyl rings is linked to an aromatic Schiff base, have been synthesized and analyzed for their second-order nonlinearity (β). Two photon fluorescence corrected β, of these complexes correlates well with the electron withdrawing nature of the substituted benzene ring. The well-known two-state model has been invoked to rationalize the observed values of the first hyperpolarizability, β, of these complexes. The metal to ligand charge transfer (MLCT) transition dominates their second-order response. These compounds form charge transfer (CT) complexes with acceptors such as iodine, *p*-chloranil (CA), 2, 3-dichloro-5, 6-dicyano-1, 4-benzoquinone (DDQ), tetracyanoethylene (TCNE), and 7, 7, 8, 8-tetracyanoquinodimethane (TCNQ). The CT complexes exhibit much higher second-order response. A series of bisferrocenyl complexes where two ferrocene moieties are linked through the same aromatic Schiff base spacer has also been synthesized and characterized. The β values of the bisferrocenyl complexes and their CT counterparts are much higher than the corresponding monoferrocene complexes. In all these compounds there is a strong resonant contribution to β due to the MLCT transition around 532 nm. The dispersion free hyperpolarizability, β_0 of these complexes have also been calculated using the two-state model.

Keywords: Ferrocene; Charge-transfer; Nonlinear optics; Ferrocene; Schiff-base

1. Introduction

Since the report [1] that ferrocene derivatives namely *trans*-1-ferrocenyl-2-(*N*-methylpyridinium-4-yl)ethylene iodide and *trans*-1-ferrocenyl-2-(4-nitrophenyl) ethylene have excellent second harmonic generation efficiencies (220 and 62 times that of urea, respectively), metallocene based complexes have been studied extensively for second-order nonlinear optics (NLO) [2,3]. The large hyperpolarizabilities in these molecules are attributed to the facile redox changes that are possible at the metal center and the presence of an extended π electron framework. Kanis et al. [4] have studied quadratic hyperpolarizabilities of ferrocene based π-systems theoretically using Zerner intermediate neglect of differential overlap-sum over excited particle-hole states (ZINDO-SOS) quantum chemical calculations. In accord with the traditional design rules based on conjugated organic molecules, they observed that enhanced electron delocalization in the ferrocenyl complex leads to greater second-order nonlinearity. The ZINDO-SOS calculations indicate that two metal to ligand charge transfer (MLCT) transitions, originating from the iron in ferrocene, are primarily responsible for second harmonic generation in these chromophores. Based on their calculations they inferred that organometallic chromophores must possess a highly polarized ligation sphere around the metal ion for effective second-order response. Detailed calculations, photoelectron spectra, and electrochemistry have been used to study the electronic structure of a series of metallocenes coupled to organic dyes by Barlow et al. [5]. Several new systems containing a metallocene unit as a donor have been studied [5–12]. Jayprakash et al. [7] have reported large second-order nonlinearity in organometallic polyene complexes containing ferrocene as a donor and a Fischer carbene complexed to a metal center (Cr or W) as an acceptor. Balavoine et al. [10] have found large

* Corresponding author. Tel.: +91-80-3092663; fax: +91-80-3600683.

E-mail address: ashoka@ipc.iisc.ernet.in (A.G. Samuelson).

0022-328X/00/$ - see front matter
PII: S0022-328X(00)00278-3

macroscopic nonlinearity in a new class of chiral ferrocenyl materials. Campo et al. [11] have reported large macroscopic nonlinearities in bent ferrocenyl systems where ferrocene is a donor. Hendrickx et al. [12] have measured moderate β values in some bimetallic monocation π-complexes of iron with ferrocene as a donor at one end of an alkyne spacer.

Thus all the previous investigations on ferrocene based complexes, both experimental and theoretical lead to the following guidelines for designing organometallic ferrocene compounds with enhanced second-order optical nonlinearity. They are: (1) the low energy MLCT band of the ferrocene moiety must be exploited; (2) the ligation sphere around the Fe-core should be made highly polarizable by either chemical modifications or external means; and (3) a significant difference in the amount of charge transfer between the donor and acceptor in the ground and excited states must be achieved. Recently Coe et al. [13] have investigated another possibility in transition metal complexes namely variation of the metal oxidation states in ruthenium bipyridyl complexes. They have demonstrated the exciting possibility of redox switching in NLO response. However, very little is known about ligand to metal charge transfer excitations and ligand to acceptor–solvent charge transfer excitations in metallocenes, and these might also be important in the context of second-order NLO. Situations are conceivable in which charge transfer through oxidation or reduction of the metallocene π-electron network could lead to a very high second-order response.

In this contribution, we explore the molecular hyperpolarizability of a series of complexes where a ferrocene unit is attached to a substituted benzene moiety through a Schiff base linkage. The resulting ferrocenyl complexes (Fig. 1) have been used as donors to prepare charge transfer (CT) compounds with a variety of organic acceptors. A similar series of bisferrocenyl complexes and their CT counterparts have also been synthesized and their β values measured. A preliminary communication of some of these results has appeared [8]. The dispersion-free hyperpolarizabilities, β_0 of these complexes have also been calculated using the two-state model [14]. The CT complexes do not exhibit significantly different β_0 values compared to the starting materials. No significant solvatochromic shift of the UV–vis absorption bands has been observed in the neutral complexes as in the case of gold complexes studied by Whittall et al. [15]. The two-state model appears to explain qualitatively the observed hyperpolarizability in these molecules.

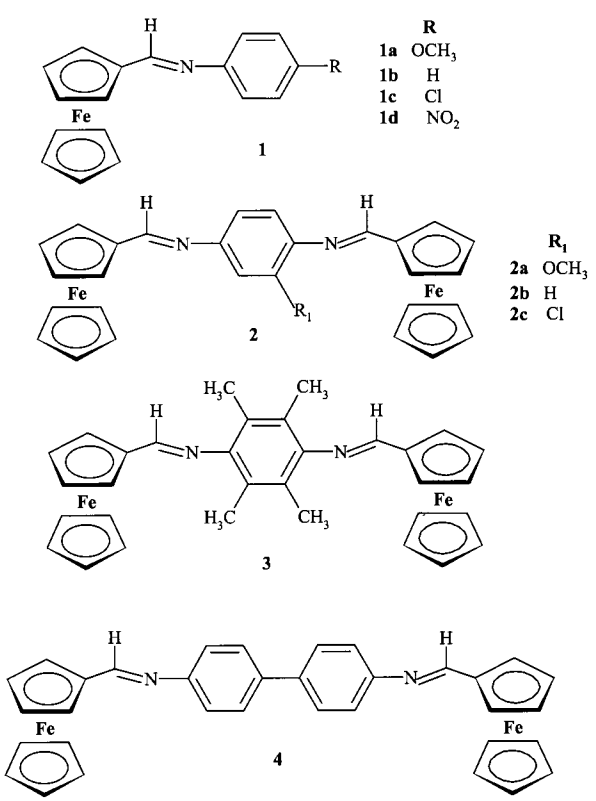

Fig. 1. Structures of compounds **1**–**4**.

2. Experimental

2.1. Physical measurements

C, H, N analysis of the complexes were obtained from Carlo Erba Strumentazione elemental analyzer-model 1106. The IR spectra of the complexes were recorded using a Bio Rad FT IR, FTS-7 spectrometer in the range 400–4000 cm^{-1} in a KBr disc. UV–vis spectra of the complexes were recorded on a Hitachi U-3400 spectrophotometer. ^{1}H- and ^{13}C-NMR spectra of the complexes were recorded using a Bruker ACF 200 FT NMR spectrometer. Cyclic voltammograms of the complexes 1–4 were recorded in a EG & G PAR model 174A polarographic analyzer combined with a standard three electrode configuration. A platinum or a glassy carbon electrode was used as the working electrode and the counter electrode was a platinum wire. A standard calomel electrode was used as a reference electrode. In all electrochemical measurements 0.1 M Bu_4NClO_4 (TBAP) was used as a supporting electrolyte and the redox potentials of the complexes were measured against the saturated calomel electrode.

2.2. Synthesis of Fc–CH=N–C_6H_4–R(p) [R = OCH_3 (1a); Cl (1c); NO_2 (1d)]

The synthetic procedure for the preparation of complexes **1a**, **1c**, and **1d** is similar. Ferrocenecarboxaldehyde was dissolved in dry toluene. The corresponding amine was added and the reaction mixture was refluxed

for 20 h. Then it was cooled to room temperature (r.t.) and filtered. The filtrate was evaporated to dryness completely. The residue was dissolved in 1:1 dichloromethane–hexane mixture and crystalized. Finally it was filtered and washed with hexane and dried under vacuum. Yield of **1a**, **1c** and **1d** are 72, 80 and 71%, respectively. Anal. Found (Calc.) for $C_{18}H_{17}FeNO$ (**1a**): C, 67.33 (67.73); H, 5.69 (5.37); N, 3.91 (4.39). For $C_{17}H_{14}NClFe$ (**1c**): C, 62.87 (63.09); H, 4.22 (4.36); N, 3.62 (3.33). For $C_{17}H_{14}N_2O_2Fe$ (**1d**): C, 61.78 (61.10); H, 4.01 (4.22); N, 8.67 (8.38)%. IR data (cm^{-1}): Complex **1a**: 3092(w), 2956(w), 2834(w), 1619(m), 1510(vs), 1246(vs), 1031(m), 820(m). Complex **1c**: 1620(s), 813(w). Complex **1d**: 3129(w), 1615(m), 1597(m), 1578(s), 1336(vs), 1103(m), 822(w), 742(w). ^{1}H-NMR spectra ($CDCl_3$): Complex **1a**, 8.33 (s, 1H, CH=N), 7.12–7.16 (m, 2H, Ph), 6.88–6.93 (m, 2H, Ph), 4.78 (t, 2H, C_5H_4), 4.47 (t, 2H, C_5H_4), 4.24 (s, 5H, C_5H_5), 3.83 (s, 3H, OCH_3). Complex **1c**: 8.30 (s, 1H, CH=N), 7.30–7.35 (m, 2H, Ph), 7.05–7.11 (m, 2H, Ph), 4.79 (t, 2H, C_5H_4), 4.51 (t, 2H, C_5H_4), 4.25 (s, 5H, C_5H_5). Complex **1d**: 8.35 (s, 1H, CH=N), 8.21–8.28 (m, 2H, Ph), 7.15–7.22 (m, 2H, Ph), 4.83 (t, 2H, C_5H_4), 4.58 (t, 2H, C_5H_4), 4.28 (s, 5H, C_5H_5). ^{13}C-NMR spectra. Complex **1a**: 55.36 (OCH_3), 68.71 (2,2′ Cp), 69.05 (Cp, s), 70.89 (3,3′ Cp), 80.67 (1, Cp), 114.23 (C_6H_4), 121.53 (C_6H_4), 145.87 (C_6H_4), 157.49 (C_6H_4), 159.42 (CH=N). Complex **1c**: 69.32 (Cp), 69.48 (Cp), 71.62 (Cp), 80.38 (Cp), 122.12 (C_6H_4), 129.29 (C_6H_4), 130.61 (C_6H_4), 151.49 (C_6H_4), 161.72 (CH=N). Complex **1d**: 69.31 (Cp), 71.95 (Cp), 72.95 (Cp), 79.25 (Cp), 120.82 (C_6H_4), 124.87 (C_6H_4), 144.77 (C_6H_4), 158.39 (C_6H_4), 163.75 (CH=N).

2.3. Synthesis of Fc–CH=N–$C_6H_3(OCH_3)$–N=CH–Fc (2a)

Ferrocenecarboxaldehyde (0.428 g, 2 mmol) and 2,5-diamino anisole (0.138 g, 1 mmol) were dissolved in 75 ml of toluene. A catalytic amount of *p*-toluene sulfonic acid (10 mmol%) was added to the reaction mixture. The reaction flask was connected to a condenser equipped with a Dean–Stark apparatus. The wine-red solution was then refluxed with azeotropic removal of water under nitrogen atmosphere. After 16 h the refluxing was stopped and the mixture was hot filtered. The filtrate was concentrated to dryness under reduced pressure. The crude product was washed with ethanol, then with petroleum ether and air dried to give 0.32 g of **2a**. Yield: 61%. Anal. Found (Calc.) for $C_{29}H_{26}Fe_2N_2O$ (**2a**): C, 64.69 (65.69); H, 5.09 (4.94); N, 4.69 (5.28)%. IR (KBr, cm^{-1}): 2920(w), 1623(vs), 1464(m), 1104(m), 1035(m), 813(s), 505(m). ^{1}H-NMR ($CDCl_3$): 3.91 (s, 3H, OCH_3), 4.27 (s, 10H, C_5H_5), 4.49 (t, 4H, C_5H_4), 4.81 (t, 4H, C_5H_4), 6.74–6.80 (m, 2H, C_6H_3), 6.96 (d, 1H, C_6H_3), 8.34 (s, 1H, –CH=N–), 8.39 (s, 1H, –CH=N–) ppm. ^{13}C-NMR (200 MHz, $CHCl_3$): 55.67 (OCH_3), 68.83 (Cp, 2-2′), 69.11 (Cp), 71.08 (Cp, 3-3′), 80.36 (Cp, 1), 105.41 (C_6H_3), 111.57 (C_6H_3), 120.59 (C_6H_3), 140.13 (C_6H_3), 150.59 (C_6H_3), 152.10 (C_6H_3), 160.22 (–CH=N–), 161.84 (–CH=N–).

2.4. Synthesis of Fc–CH=N–$C_6H_3(Cl)$–N=CH–FC (2c)

To a solution of ferrocenecarboxaldehyde (0.89 g, 4.14 mmol) in 100 ml of toluene were added 2-chloro-1,4-phenylenediamine (0.29 g, 2.07 mmol) and a catalytic amount of *p*-toluene sulfonic acid (10 mol%). The reaction mixture was heated to reflux and azeotropic removal of water was accomplished using a Dean–Stark apparatus. After 20 h the solution was filtered and evaporation of the solvent gave a red oily substance which was dissolved in a small quantity of dichloromethane and layered with petroleum ether. On standing overnight, dark red colored crystals separated out, which were washed with ethanol and petroleum ether to give 0.55 g of **2c**. Yield: 62%. Anal. Found (Calc.) for $C_{28}H_{23}ClFe_2N_2$ (**2c**): C, 62.84 (62.90); H, 4.67 (4.34); N 5.42 (5.24)%. IR (KBr, cm^{-1}): 3080(w), 1619(vs), 1455(w), 1105(w), 1037(w), 806(s), 516(m). ^{1}H-NMR ($CDCl_3$): 4.27 (s, 5H, C_5H_5), 4.28 (s, 5H, C_5H_5), 4.51 (q, 4H, C_5H_4), 4.80 (t, 2H, C_5H_4), 4.84 (t, 2H, C_5H_4), 6.98 (d, 1H, C_6H_3), 7.06 (q, 1H, C_6H_3), 7.24 (q, 1H, C_6H_3), 8.28 (s, 1H, –CH=N–), 8.36 (s, 1H, –CH=N–) ppm. ^{13}C-NMR (200 MHz, $CHCl_3$): 68.68 (Cp, 2-2′), 69.15 (Cp), 69.32 (Cp, 3-3′), 70.93 (Cp, 2-2′), 71.31 (Cp), 73.50 (Cp, 3-3′), 79.85 (Cp, 1), 80.10 (Cp, 1), 115.98 (C_6H_3), 120.44 (C_6H_3), 121.44 (C_6H_3), 147.55 (C_6H_3), 150.12 (C_6H_3), 158.95 (C_6H_3), 161.13 (–CH=N–), 162.62 (–CH=N–).

2.5. Synthesis of Fc–CH=N–$C_6(Me_4)$–N=CH–Fc (3)

Ferrocenecarboxaldehyde (0.214 g, 1 mmol) and 2,3,5,6-tetramethyl-1, 4-phenylenediamine (0.082 g, 0.5 mmol) were dissolved in toluene (75 ml) with a catalytic amount of *p*-toluene sulfonic acid (10 mmol%). The reaction flask was connected to a condenser equipped with a Dean–Stark apparatus. The wine red solution was then refluxed for 20 h. The hot solution was filtered and the filtrate was concentrated to dryness in a rotary evaporator. Washing with ethanol to remove unreacted starting materials left an orange solid which was air dried to give **3** (0.401 g, yield: 72%). Anal. Found (Calc.) for $C_{32}H_{32}Fe_2N_2$ (**3**): C, 68.89 (69.09); H, 5.68 (5.79); N, 5.10 (5.04)%. IR (KBr, cm^{-1}): 3073(w), 2857(w), 1628(vs), 1456(s), 1410(s), 1239(s), 1105(m), 827(s), 502(m). ^{1}H-NMR ($CDCl_3$): 2.11 (s, 12H, CH_3), 4.28 (s, 10H, C_5H_5), 4.48 (t, 4H, C_5H_4), 4.81 (t, 4H, C_5H_4), 8.02 (s, 2H, –CH=N–) ppm. ^{13}C-NMR (200 MHz, $CHCl_3$): 14.88 (CH_3), 68.51 (Cp, 2-2′), 68.88 (Cp), 70.62 (Cp, 3-3′), 80.92 (Cp, 1), 123.26 (phenyl carbon), 148.12 (phenyl carbon), 162.94 (–CH=N–).

2.6. Synthesis of Fc–CH=N–C_6H_4–C_6H_4–N=CH–Fc (4)

Synthesis of **4** was carried out using a procedure identical to the synthesis of **3** starting with formyl ferrocene and benzidene. Yield: 80%. Anal. Found (Calc.) for $C_{34}H_{28}Fe_2N_2$ (**4**): C, 70.76 (70.86); H, 4.74 (4.89); N, 4.92 (4.86)%. IR (KBr, cm^{-1}): 3071(vw), 1618(vs), 1592(vs), 1489(s), 1462(s), 1260(m), 1105(m), 811(s), 502(m). ^{1}H-NMR ($CDCl_3$): 4.26 (s, 10H, C_5H_5), 4.50 (t, 4H, C_5H_4), 4.82 (t, 4H, C_5H_4), 7.23–7.63 (m, 8H, phenyl ring proton), 8.40 (s, 2H, –CH=N–) ppm. ^{13}C-NMR (200 MHz, $CHCl_3$): 69.17 (Cp, 2-2′), 69.37 (Cp), 71.39 (Cp, 3-3′), 80.58 (Cp, 1), 121.19 (phenyl, 3-3′), 127.61 (phenyl, 2-2′), 137.82 (phenyl, 1-1′), 151.92 (phenyl, 4-4′), 161.17 (–CH=N–).

2.7. Preparation of the charge transfer complexes

The ferrocene containing Schiff base was dissolved in a small quantity of chloroform (benzene in the case of the TCNE complex). The acceptors were dissolved in chloroform (benzene in the case of TCNE and acetonitrile in the case of TCNQ) and added from a dropping funnel into the stirred solution of the Schiff base at r.t. over a period of 0.5–1 h. After the addition was complete the reaction mixture was stirred at r.t. for 12–14 h. During the course of the reaction the CT complexes were precipitated from the solution which was removed by filtration. The precipitate was washed with chloroform or benzene (for TCNE complex) in order to remove the unreacted starting materials. A final drying under vacuum gave analytically pure material.

2.7.1. Characterization of [Fc–CH=N–$C_6H_3(OCH_3)$–N=CH–Fc] I_5

Yield: 46.1%. Anal. Found (Calc.) for $C_{29}H_{26}Fe_2I_5N_2O$: C, 29.95 (29.90); H, 2.12 (2.25); N, 2.41 (2.41)%. IR data (cm^{-1}): 3077(w), 1617(vs), 1586(s), 1514(s), 1344(s), 1024(w), 826(s), 498(w).

2.7.2. Characterization of [Fc–CH=N–$C_6H_3(OCH_3)$–N=CH–Fc] $(DDQ)_2$

Yield: 71.4%. Anal. Found (Calc.) for $C_{45}H_{26}Cl_4Fe_2N_6O_5$: C, 55.12 (54.91); H, 2.58 (2.67); N, 8.44 (8.54)%. IR data (cm^{-1}): 3386(w, br), 2227(w), 1653(s), 1600(s), 1515(m), 1413(vs), 1278(w), 905(w), 833(w).

2.7.3. Characterization of [Fc–CH=N–$C_6H_3(OCH_3)$–N=CH–Fc] $(TCNE)_2$

Yield: 13.6%. Anal. Found (Calc.) for $C_{41}H_{26}Fe_2N_{10}O$: C, 62.79 (62.61); H, 3.48 (3.34); N 18.04 (17.81)%. IR data (cm^{-1}): 3107(w), 2203(s), 1644(s), 1581(vs), 1514(s), 1350(m), 1028(w), 830(w), 682(w), 503(w).

2.7.4. Characterization of [Fc–CH=N–$C_6H_3(OCH_3)$–N=CH–Fc] $(TCNQ)_2$

Yield: 64.1%. Anal. Found (Calc.) for $C_{53}H_{34}Fe_2N_{10}O$: C, 67.87 (67.81); H, 3.59 (3.66); N 15.03 (14.93)%. IR data (cm^{-1}): 2188(m), 1655(s, br), 1506(w), 1327(w), 1203(s), 1145(s), 837(w), 724(w).

2.7.5. Characterization of [Fc–CH=N–$C_6H_3(OCH_3)$–N=CH–Fc] $(CA)_2$

Yield: 21.7%. Anal Found (Calc.) for $C_{41}H_{26}Cl_8Fe_2N_2O_5$: C, 48.02 (48.18); H, 2.55 (2.57); N, 2.69 (2.74)%. IR data (cm^{-1}): 3327(s), 1641(s), 1613(s), 1573(vs), 1513(vs), 1463(s), 1294(s), 1217(m), 1028(w), 832(w), 500(w).

2.7.6. Characterization of [Fc–CH=N–$C_6H_3(Cl)$–N=CH–Fc] $I_{4.5}$

Yield: 53.3%. Anal. Found (Calc.) for $C_{28}H_{23}ClFe_2I_{4.5}N_2$: C, 30.29 (30.41); H, 2.11 (2.09); N, 2.58 (2.53)%. IR data (cm^{-1}): 3357(w), 3081(w), 1634(vs), 1571(s), 1511(s), 1470(s), 1319(m), 819(w), 496(w).

2.7.7. Characterization of [Fc–CH=N–$C_6H_3(Cl)$–N=CH–Fc] $(DDQ)_4$

Yield: 44.0%. Anal. Found (Calc.) for $C_{60}H_{23}Cl_8Fe_2N_{10}O_8$: C 49.99 (49.95); H 1.94 (1.61); N 9.66 (9.71)%. IR data (cm^{-1}): 3214(w, br), 2227(w), 1626(s), 1574(s), 1505(w), 1453(s), 1411(w), 1277(w), 1198(w), 1000(w), 829(w).

2.7.8. Characterization of [Fc–CH=N–$C_6H_3(Cl)$–N=CH–Fc] $(TCNE)_2$

Yield: 12.6%. Anal. Found (Calc.) for $C_{40}H_{23}ClFe_2N_{10}$: C, 60.93 (60.75); H, 2.90 (2.93); N, 17.52 (17.71)%. IR data (cm^{-1}): 2208(s), 2188(s), 1661(s), 1629(s), 1583(vs), 1478(s), 1322(w), 820(s).

2.7.9. Characterization of [Fc–CH=N–$C_6H_3(Cl)$–N=CH–Fc] $(TCNQ)_2$

Yield: 53.8%. Anal. Found (Calc.) for $C_{52}H_{31}ClFe_2N_{10}$: C, 66.44 (66.23); H, 3.41 (3.31); N 14.62 (14.85)%. IR data (cm^{-1}): 3050(w), 2186(w), 1703(m), 1626(s), 1603(s), 1505(s), 1413(w), 1315(w), 1186(w), 823(w).

2.7.10. Characterization of [Fc–CH=N–$C_6H_3(Cl)$–N=CH–Fc] $(CA)_2$

Yield: 14.8%. Anal. Found (Calc.) for $C_{40}H_{23}Cl_9Fe_2N_2O_4$: C, 46.95 (46.81); H, 2.49 (2.26); N, 2.72 (2.72)%. IR data (cm^{-1}): 3365(w), 1623(s), 1575(s), 1505(s), 1312(w), 827(w).

2.7.11. Characterization of [Fc–CH=N–$C_6(CH_3)_4$–N=CH–Fc] I_3

Yield: 50.9%. Anal. Found (Calc.) for $C_{32}H_{32}Fe_2I_3N_2$: C, 41.53 (41.02); H, 3.58 (3.44); N, 2.77 (2.99)%.

IR data (cm^{-1}): 3083(w), 2920(w), 1617(vs), 1454(m), 1244(m), 1036(m), 1000(m), 827(s), 681(m).

2.7.12. Characterization of
[Fc–CH=N–$C_6(CH_3)_4$–N=CH–Fc] $(DDQ)_2$

Yield: 86.9%. Anal. Found (Calc.) for $C_{48}H_{32}Cl_4Fe_2N_6O_4$: C, 57.29 (57.06); H, 3.08 (3.19); N, 7.92 (8.32)%. IR data (cm^{-1}): 3111(w), 3013(w), 2231(m), 1677(s), 1629(s), 1559(s), 1415(vs), 1268(s), 1095(m), 910(w), 827(w), 484(w).

2.7.13. Characterization of
[Fc–CH=N–$C_6(CH_3)_4$–N=CH–Fc] $(TCNE)_2$

Yield: 29.5%. Anal. Found (Calc.) for $C_{44}H_{32}Fe_2N_{10}$: C, 65.19 (65.04); H, 4.08 (3.97); N, 16.98 (17.24)%. IR data (cm^{-1}): 3348(m), 3248(m), 2202(s), 1633(s), 1594(vs), 1504(s), 1107(w), 830(w).

2.7.14. Characterization of
[Fc–CH=N–$C_6(CH_3)_4$–N=CH–Fc] $(TCNQ)_2$

Yield: 57.1%. Anal. Found (Calc.) for $C_{56}H_{40}Fe_2N_{10}$: C, 69.58 (69.72); H, 4.32 (4.18); N, 14.44 (14.52)%. IR data (cm^{-1}): 3399(w), 3050(w), 2184(vs), 2158(m), 1634(s), 1579(m), 1505(m), 1180(m), 830(w).

2.7.15. Characterization of
[Fc–CH=N–$C_6(CH_3)_4$–N=CH–Fc] $(CA)_3$

Yield: 37.1%. Anal. Found (Calc.) for $C_{50}H_{32}Cl_{12}Fe_2N_2O_6$: C, 46.23 (46.23); H, 2.63 (2.49); N, 2.23 (2.16)%. IR data (cm^{-1}): 3395(w), 3092(w), 2922(w), 1678(m), 1628(vs), 1584(m), 1554(m), 1456(m), 1245(w), 1106(w), 827(w).

2.7.16. Characterization of
[Fc–CH=N–C_6H_4–C_6H_4–N=CH–Fc] I_3

Yield: 38.1%. Anal. Found (Calc.) for $C_{34}H_{28}Fe_2I_3N_2$: C, 42.34 (42.67); H, 3.22 (2.95); N, 3.03 (2.93)%. IR data (cm^{-1}): 3080(w), 1628(vs), 1582(m), 1466(m), 1345(m), 1106(w), 820(s).

2.7.17. Characterization of
[Fc–CH=N–C_6H_4–C_6H_4–N=CH–Fc] $(DDQ)_2$

Yield: 89.7%. Anal. Found (Calc.) for $C_{50}H_{28}Cl_4Fe_2N_6$: C, 58.24 (58.28); H, 2.54 (2.74); N, 8.36 (8.16)%. IR data (cm^{-1}): 2222(w), 1639(s), 1607(m), 1573(s), 1498(s), 1407(s), 1004(w), 903(w), 825(w).

2.7.18. Characterization of
[Fc–CH=N–C_6H_4–C_6H_4–N=CH–Fc] $(TCNE)_2$

Yield: 21.8%. Anal. Found (Calc.) for $C_{46}H_{28}Fe_2N_{10}$: C, 66.54 (66.36); H, 3.31 (3.40); N, 16.95 (16.83)%. IR data (cm^{-1}): 2197(w), 1645(s), 1567(s), 1474(m), 1350(w), 1003(w), 826(w).

2.7.19. Characterization of
[Fc–CH=N–C_6H_4–C_6H_4–N=CH–Fc] $(TCNQ)_2$

Yield: 30.9%. Anal. Found (Calc.) for $C_{58}H_{32}Fe_2N_{10}$: C, 71.39 (71.03); H, 3.38 (3.30); N, 14.24 (14.29)%. IR data (cm^{-1}): 3434(w), 3353(s), 3239(w), 2213(s), 2178(m), 2133(w), 1650(m), 1607(s), 1563(m), 1501(s), 1413(m), 1178(m), 823(w).

2.7.20. Characterization of
[Fc–CH=N–C_6H_4–C_6H_4–N=CH–Fc] $(CA)_2$

Yield: 16.7%. Anal. Found (Calc.) for $C_{46}H_{28}Cl_8Fe_2N_2O_4$: C, 51.93 (51.73); H, 2.61 (2.65); N, 2.75 (2.62)%. IR data (cm^{-1}): 1636(m), 1605(m), 1571(s), 1498(s), 1309(w), 1005(w), 822(w).

2.8. HRS measurements

The first hyperpolarizability, β, was measured in acetonitrile by the hyper-Rayleigh scattering (HRS) technique [16,17]. The experimental set-up has been described in detail elsewhere [18]. In brief, the fundamental of a Q-switched Nd:YAG laser (Spectra Physics, 8 ns) is focused 5 cm away after passing through a glass cell containing the solute in solution. The scattered light was allowed to pass through a monochromator (Czerny–Turner, 0.25 m) and collected on a photomultiplier tube (PMT). The signal from the PMT was amplified 125 times (SRS 440), averaged over 100 shots and displayed on a digital storage oscilloscope. The signal intensity was collected as a function of wavelength from ca. 500–650 nm. Experimental data points were fitted to a Lorentzian for the second harmonic peak (532 nm) and to a Gaussian for the two-photon fluorescence (TPF) peak [19,20] wherever observed. Multiple Gaussians were also necessary in a few cases where more than one TPF peak was observed. All data were collected at laser power ≤ 24 mJ per pulse. The intensity of the second harmonic scattered light, $I_{2\omega}$ (taken from the peak of the Lorentzian fit) for a two component mixture of a solvent and a solute is given by [16]

$$I_{2\omega} = G\{N_{\text{solvent}}\cdot\beta^2_{\text{solvent}} + N_{\text{solute}}\cdot\beta^2_{\text{solute}}\}\cdot I^2_{\omega} \quad (1)$$

The quadratic coefficient $I_{2\omega}/I^2_{\omega}$ varies linearly with the number density, N_{solute} of the solute, if β and N for the solvent are fixed. The proportionality factor G is obtained from the intercept of this linear plot when β_{solvent} is known. This is the well-known internal reference method. Since low concentrations (10^{-5} to 10^{-6} M) of solute were used, we assume that the presence of the solute molecules does not change the number density of the solvent molecules, N_{solvent}, significantly. First the β value of *p*-nitroaniline (pNA) (purchased from Aldrich and purified by repeated recrystallization from ethanol) was measured as $(23.0 \pm 2.2) \times 10^{-30}$ esu in acetonitrile which is in good agreement with the value obtained

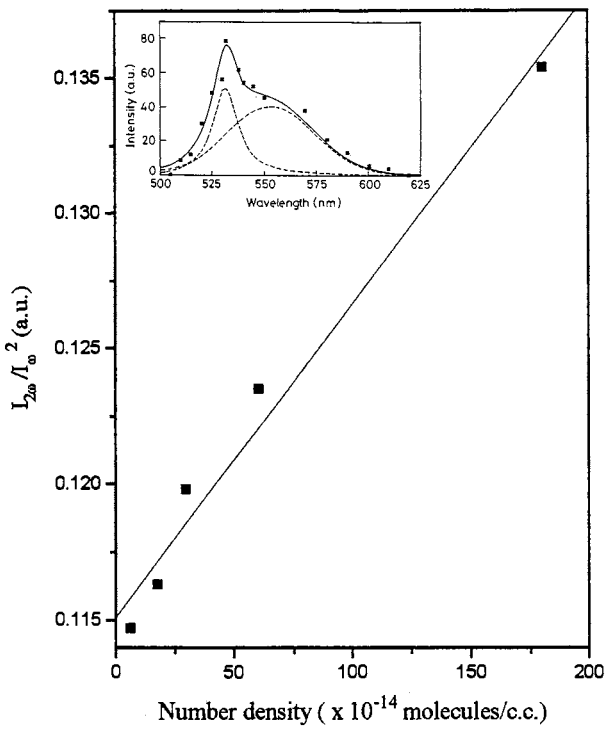

Fig. 2. $I_{2\omega}/I_{\omega}^{2}$ vs. number density of CT complex **2b**·$(TCNQ)_2$ in acetonitrile. Inset shows second harmonic spectra with TPF for the same CT complex. Experimental data points (◆); Gaussian fit to TPF (···); Lorentzian fit to HRS (- - -); and sum of the two peaks (total intensity) (—).

Table 1
λ_{max} in nm with molar extinction coefficient for the longer wavelength transition, ε ($\times 10^{-3}$) in M^{-1} cm^{-1} in parentheses, and extinction coefficient, ε ($\times 10^{-3}$) in M^{-1} cm^{-1} at 532 nm, β ($\times 10^{30}$) in esu, β_0 ($\times 10^{30}$) in esu, and redox potential, $E_{1/2}$ in V for all the neutral compounds and acceptors

Compound	λ_{max} ($\varepsilon \times 10^{-3}$)	ε_{532}	β	β_0	$E_{1/2}$
1a	326, 457 (1.36)	2.46	11.9	2.5	0.55
1b	309, 448 (2.21)	0.95	13.8	3.3	0.59
1c	316, 463 (0.93)	0.36	20.9	4.1	0.60
1d	336, 490 (1.76)	0.99	51.2	6.1	0.62
2a	356, 453 (1.06)	0.50	18.3	4.1	0.51
2b	350, 460 (9.30)	4.00	22.9	4.7	0.55
2c	348, 474 (2.39)	0.28	33.1	5.5	0.59
3	337, 455 (3.75)	1.44	22.7	4.9	0.54
4	345, 465 (4.71)	1.94	35.9	6.9	0.54
I_2	464 (0.79)	0.29	0	0	0.65
DDQ	281 (16.33)	0.88	17.1	11.5	0.55
TCNE	272 (14.27)	0.33	11.6	8.0	0.25
TCNQ	394 (49.18)	0.75	27.6	10.7	0.21
p-CA	368 (10.64)	0.40	16.8	7.7	0.03

from the electric field induced second harmonic generation (EFISHG) technique earlier (29.2×10^{-30} esu) [21]. Fig. 2 shows the plot of $I_{2\omega}/I_{\omega}^{2}$ vs. N_{solute} for the compound **2b**·$(TCNQ)_2$, in acetonitrile. At the low solute concentrations employed in our study, the plot remains linear. From the intercept and slope we have found $\beta = 143.6 \times 10^{-30}$ esu. Similarly, we have obtained β for the other neutral and CT compounds.

3. Results

The redox potentials of the various acceptors and substituted ferrorcenes have been recorded in acetonitrile. The reduction potentials of the acceptors allow us to arrange them in the order of their oxidizing ability in acetonitrile in which the β measurements were made. The redox potentials of the acceptors and the substituted ferrocenes are within experimental error of literature values. [22–24] Based on the elemental analysis, the various CT complexes formed with the acceptors were formulated to have one, two or many moles of the acceptor per ferrocene unit. The reduced species formed by the acceptors vary from one ferrocenyl system to another as indicated by the stoichiometry of the CT complexes. Although, surprising, the non-integral ratio of charge transfer complexes with iodine has been reported before [25,26] in the reaction of substituted ferrocenes with iodine. Formation of the CT adducts result in characteristic changes in the electronic and vibrational spectra of the complexes. The characteristic ⊥ C–H bend of ferrocene shifts on formation of CT adducts by 10–25 cm^{-1}. Similarly, the characteristic C=N stretch shifts on CT complex formation to different extents depending on the oxidant.

The microscopic hyperpolarizability (β) of the neutral compounds **1**–**4** and the acceptors are listed in Table 1 along with the λ_{max} and ε_{532} for all the compounds after correcting for two photon fluorescence. Using the well-known two-state model [14], dispersion free first hyperpolarizability, β_0, for these molecules were obtained and the values are included in Table 1. Molecules having longer π-conjugation have larger β as expected. The measured β shows more than 4-fold increase in the series of monoferrocenyl complexes ranging from 11.9 for the methoxy substituted monoferrocenyl complex to 51.2 for the corresponding nitro substituted compound. Similarly, β for the bisferrocenyl complexes increases almost 2-fold in the series from 18.3 to 33.1. However, the corresponding β_0, varies over a narrower range from 2.5 to 7.

The hyperpolarizability, β for the CT compounds shows a much greater variation, from 53.5, measured for the TCNQ adduct of complex **1b**, to 288.1 for the TCNE adduct of **4**. The measured β, λ_{max}, ε_{532} and β_0 for the CT complexes of **1**–**4** are given in Table 2(a–f). Unlike the neutral compounds, there is a large variation in β as well as β_0 in the CT complexes. The latter varies from 2.6 for the CT complex of **1b** with I_2 to 52.5 for the CT complex of **2c** with CA.

4. Discussion

4.1. Spectroscopic investigations

The electronic absorption spectra of ferrocene and substituted ferrocenes have been investigated intensely in the past [27,28]. In ferrocene, the d_{z^2} orbital is the HOMO, centered on the metal and a degenerate set of ligand orbitals in combination with the metal d_{xz} and d_{yz} is the LUMO. The absorption around 440 nm in ferrocene is attributed to the $^1E_{1g} \leftarrow {}^1A_{1g}$ transition. A higher energy band around 325 nm has been assigned as the $^1E_{2g} \leftarrow {}^1A_{1g}$ transition. Similarly, all the compounds examined in the present study show two characteristic bands in the UV–vis spectra (Fig. 3). One absorption band in the range of 300–400 nm and the other in the range of 450–550 nm. In compounds (**1b**–**d**) where the Schiff base with various substituents is attached to the Cp, the low-energy transition shows shifts depending on the substituent. These absorption shifts clearly indicate that the LUMO has significant contributions from the Schiff base orbitals in these complexes.

Surprisingly the spectroscopic studies on the CT adducts do not show a simple correlation of the λ_{max} with the oxidation potential of the acceptor. Representative absorption spectra are shown in Fig. 4. The IR spectra indicate changes in $\nu_{C=N}$ and $\perp$ C–H bend, but these shifts do not correlate with the oxidation potential of the acceptor in a linear fashion. Differences in the

Table 2
λ_{max} in nm with molar extinction coefficient for the longer wavelength transition, ε ($\times 10^{-3}$) in M^{-1} cm^{-1} in parentheses, and extinction coefficient, ε ($\times 10^{-3}$) in M^{-1} cm^{-1} at 532 nm, redox potential, $\Delta E_{1/2}$ in V, β ($\times 10^{30}$) in esu, and β_0 ($\times 10^{30}$) in esu, for all the CT compounds (a) CT complexes of **1b**; (b) CT complexes of **2a**; (c) CT complexes of **2b**; (d) CT complexes of **2c**; (e) CT complexes of **3**; and (f) CT complexes of **4**

Compound	λ_{max}	ε_{532}	$\Delta E_{1/2}$	β	β_0
a					
1b·I_3	355, 525 (2.62)	2.56	0.06	130.9	2.6
1b·$(DDQ)_2$	349, 565 (1.35)	1.64	−0.03	132.2	12.1
1b·TCNE	434, 565 (3.34)	4.07	−0.34	146.3	13.4
1b·TCNQ	393, 470 (8.49)	3.37	−0.37	53.5	9.4
1b·$(CA)_2$	435, 560 (5.04)	5.79	−0.55	221.3	17.3
b					
2a·I_5	451, 514 (5.10)	4.14	0.14	126.5	6.5
2a·$(DDQ)_2$	422, 546 (5.16)	83.39	0.05	173.5	6.8
2a·$(TCNE)_2$	374, 498 (7.41)	5.55	−0.26	259.2	25.1
2a·$(TCNQ)_2$	395, 482 (2.54)	1.49	−0.29	165.9	23.6
2a·$(CA)_2$	360, 634 (20.50)	9.88	−0.47	134.9	36.6
c					
2b·$I_{4.5}$	363, 510 (9.80)	9.36	0.09	136.6	8.5
2b·$(DDQ)_2$	417, 582 (3.61)	4.07	−0.01	149.9	20.7
2b·$(TCNE)_2$	378, 479 (11.65)	8.53	−0.31	181.2	27.3
2b·$(TCNQ)_2$	394, 476 (17.96)	8.32	−0.34	143.6	22.9
2b·$(CA)_2$	393, 570 (12.51)	13.88	−0.52	263.3	27.8
d					
2c·$I_{4.5}$	366, 521 (5.35)	5.22	0.05	159.9	4.9
2c·$(DDQ)_4$	409, 588 (3.63)	4.39	−0.04	175.0	26.9
2c·$(TCNE)_2$	373, 490 (11.59)	8.89	−0.35	125.5	33.6
2c·$(TCNQ)_2$	394, 476 (3.39)	1.89	−0.38	204.0	32.5
2c·$(CA)_2$	440, 601 (4.40)	6.59	−0.56	279.1	52.5
e					
3·I_3	359, 502 (4.91)	4.32	0.10	120.8	10.3
3·$(DDQ)_2$	362, 494 (5.34)	4.24	−0.01	152.6	16.5
3·$(TCNE)_2$	417, 478 (11.13)	6.57	−0.30	160.5	24.7
3·$(TCNQ)_2$	394, 475 (15.56)	6.31	−0.33	170.7	27.7
3·$(CA)_3$	371, 438 (2.73)	0.94	−0.51	170.1	45.5
f					
4·I_3	363, 524 (7.06)	6.95	0.10	149.4	3.4
4·$(DDQ)_2$	408, 590 (7.71)	10.72	0.01	131.8	20.9
4·$(TCNE)_2$	368, 505 (5.69)	5.31	−0.29	288.1	22.1
4·$(TCNQ)_2$	394, 478 (13.58)	6.99	−0.33	172.5	26.5
4·$(CA)_2$	356, 448 (4.14)	1.71	−0.51	196.6	47.0

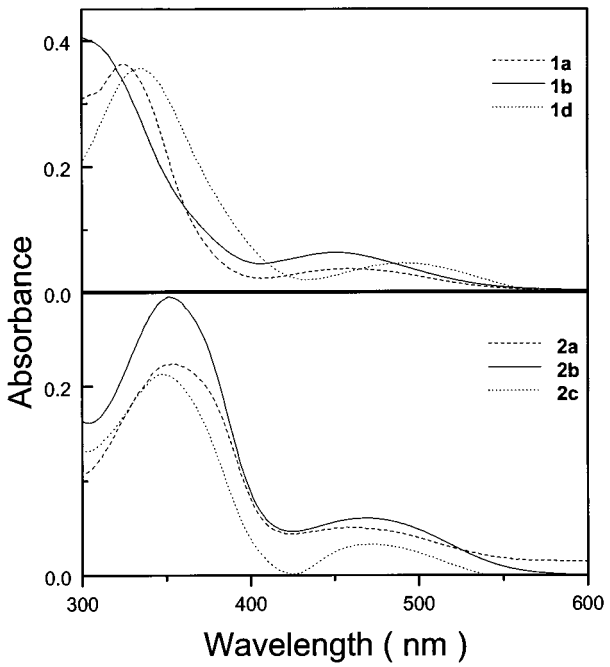

Fig. 3. Absorption spectra of compounds **1a**–**b**, **1d**, **2a**–**c** in acetonitrile.

energy, size and symmetry of the acceptor orbitals lead to different regions of charge depletion in the Schiff bases and consequently do not allow for a simple correlation with the redox potential.

4.2. First hyperpolarizability of the neutral complexes

Based on the absorption spectra, the excited state of these complexes seems to have more electron density localized on the Schiff base substitution of the Cp ligand compared to the ground state where the HOMO is almost entirely on the metal. This difference in electron density delocalization in the ground and excited states should lead to a large change in dipole moments, $\Delta\mu$ (that is, $\mu_{\text{excited state}} - \mu_{\text{ground state}}$). The situation is entirely analogous to the linking of an acceptor (A) and a donor (D) through a conjugated organic spacer resulting in an A–D motif where the excited state has a larger dipole moment relative to the ground state. Extending this idea to the ferrocenyl complexes studied here, we expect large β for molecules with: (i) extended conjugation attached to the Cp ring; and (ii) acceptor groups on the aryl ring of the spacer. Based on the inductive effect we would expect the methoxy substituted ferrocenyl complex to have a larger β than the unsubstituted compound. However, it is observed that compound **1a** has the lowest β. Addition of electron withdrawing substituents to the aryl ring attached to the Cp moiety makes the aryl ring a better acceptor. In fact, β varies from 11.9 for the *p*-methoxy substituted compound, **1a** to 51.2 for the strong electron withdrawing group containing molecule **1d**. A plot of β versus σ, the Hammett parameter of the substituent in the *para* position is shown in Fig. 5. The linearity of the plot confirms that the ferrocene moiety acts as a donor while the *p*-substituted benzene ring acts as an acceptor. The increase in β with the acceptor strength in an A–D motif is entirely consistent with previously observed variations of β in organometallic [29,30] compounds. It has been observed that in similarly substituted ferrocenes [30], addition of an electron withdrawing group on the aromatic substituent enhances β significantly.

The β measured in these complexes compare reasonably well with those reported for other ferrocene containing molecules. Calabrese et al. [30] have measured β for a complex where a ferrocene moiety is linked to *p*-nitro benzene through an olefinic double bond. The compound is very similar to **1d**. Their observed β (31×10^{-30} esu) is ca. 1.5 times lower than that of **1d**. There could be several reasons for the larger β measured in the monoferrocenyl Schiff-base complexes. The electric field induced second harmonic generation (EFISHG) technique used by Calabrese et al. [30] employed a different excitation wavelength, viz. 1907 nm for the second harmonic measurement and hence a direct comparison with their result is difficult without a clear knowledge of the dispersion characteristics of these molecules. The value of β depends strongly on the wavelength used for measurement. For example, in dioxane *p*-nitro aniline has $\beta = 16.9 \times 10^{-30}$ esu at 1064 nm, whereas β is 11.8×10^{-30} esu at 1370 nm and 9.6×10^{-30} esu at 1907 nm [31]. A second and more important reason is resonance enhancement. Compound **1d** absorbs strongly at 532 nm ($\varepsilon = 9.9 \times 10^2$ M^{-1} cm^{-1}) and subsequently the two-photon resonant contribution to β will be significant.

It should be noted that the role of the spacer in modulating β appears to be an important factor that is poorly understood. Krishnan et al. [32] have recently observed that P=N linkages in the place of C=C linkages increase the second-order response. Whereas Whittall et al. [15] have observed that in gold complexes replacement of C=C by C=N results in a significant drop in the second-order response exhibited by the molecule. A systematic study of the variation in the spacer is necessary to understand how the nature of the bridge influences β.

The major difference between the monoferrocenyl and bisferrocenyl complexes is the increase in the extent of conjugation. The measured hyperpolarizability increases by a factor of 1.5 in going from **1b** to **2b**. A significant proportion of this increase must be due to the dispersion in β since the increase in β_0 is only marginal. β_0 changes from 3.3 (**1b**) to 4.7 (**2b**). While it might be argued that **2b** appears more symmetrical than **1b**, there are several factors which lead to non cen-

trosymmetric minima on the conformational space and hence a non zero value of β in these systems. Most importantly, it should be noted that in the lowest energy conformer the arene ring is not in the same plane as the cyclopentadienyl ring due to a twisting of the C=N group to avoid non bonded interactions between the Schiff base proton and the Cp ring protons. Crystallographically characterized molecules exhibit a twist of $\sim 66°$ [33]. Attaching an electron withdrawing group to the aryl ring leads to a large β in these bisferrocenyl systems. Thus **2c** has a β of 33.1 and a β_0 of 5.5. The introduction of a methoxy group in the meta position in complex **2a** results in a lower value of β than the unsubstituted compound **2b**. Compound **3** is a part of the series formed by **2a**–**c** but the presence of four methyl groups on the central benzene ring is expected to cause steric crowding, reducing the delocalization of electrons. This is indeed true, and β of **3** is similar to that observed for the unsubstituted complex **2b**. β_0 of **3** is again similar to **2b** suggesting that the nonresonant contribution in both cases are comparable.

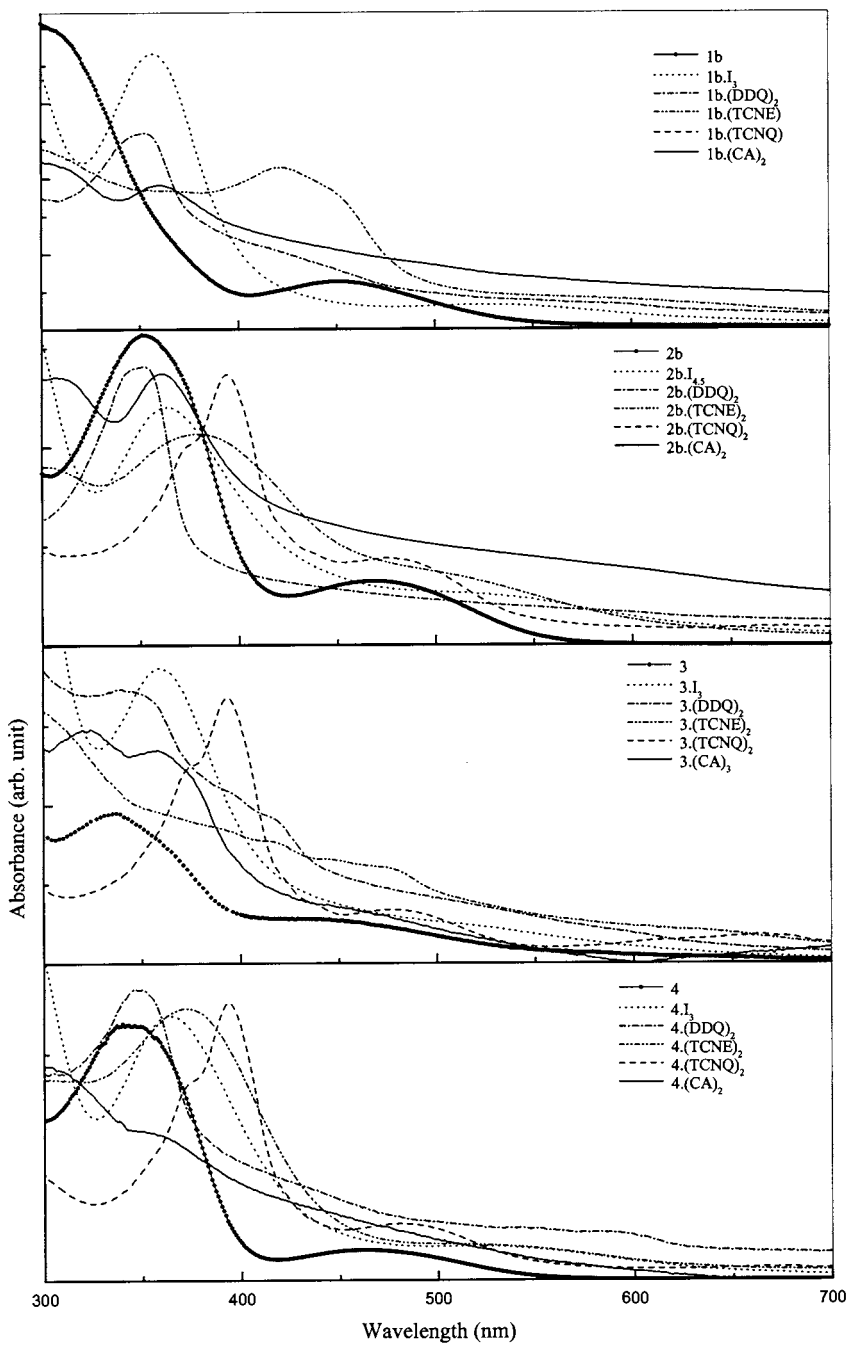

Fig. 4. Absorption spectra of CT complexes of **1b**, **2b**, **3** and **4** in acetonitrile.

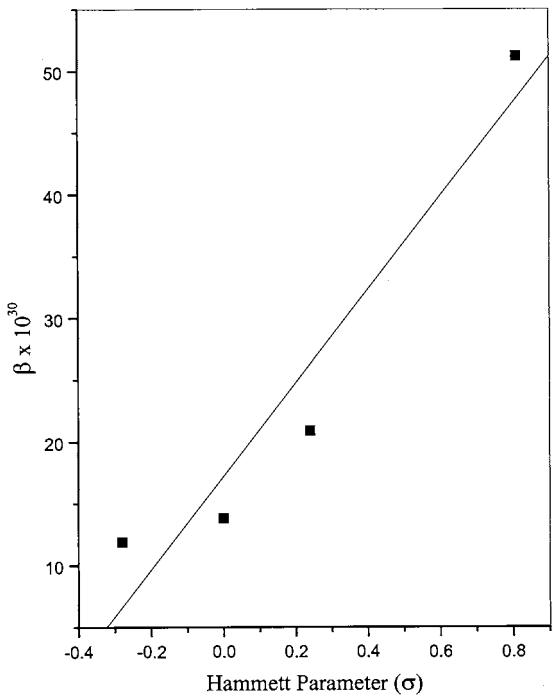

Fig. 5. First hyperpolarizability, β (in 10^{-30} esu) of compounds **1a–d** is plotted against the Hammett parameter, σ of the acceptors on the benzene ring.

From all these observations, what appears to be clearly important for obtaining a large β is the presence of extended conjugation on the substituent on the cyclopentadienyl ring. Accordingly a more significant increase in β_0 is observed in compound **4**, which has a larger π spacer between the two ferrocene units. It has been reported that for the same donor ($-NH_2$) and acceptor ($-NO_2$) pair attached to a phenyl ring in *p*-positions ($Me_2N-C_6H_4-NO_2$), β_0 is 8.2×10^{-30} esu [34], whereas when the donor and acceptor are attached to a biphenyl moiety ($Me_2N-C_6H_4-C_6H_4-NO_2$), the value of β_0 increases by a factor of 2.5 and the observed β_0 is 20×10^{-30} esu [35]. An increase (1.5 times) in β_0 is also observed in these systems, in going from complex **2b** to **4** but it is not as much as in the case of the organic donor–acceptor compound mentioned above.

Molecules **1a** to **4** have a well-defined A–D motif where the ferrocene center is the donor and the aromatic Schiff base acts as the acceptor. In this series, attaching electron withdrawing/donating groups to the aromatic ring increases/decreases β. The excited state HOMO perhaps has more ligand character when there is an electron withdrawing substituent on the benzene ring. EHT calculations have shown that the LUMO in mono and bisferrocenyl complexes has significant contribution from the substituted aromatic Schiff base attached to the Cp ring [25].

4.3. Hyperpolarizability of CT complexes

We have chosen five different acceptors having different redox potentials ($E_{1/2}$ox) for making CT complexes. While many acceptors form CT complexes with these molecules, only those that formed solid adducts were chosen to enable better characterization. It was observed that only acceptors which had a redox potential above 0.01 V versus SCE formed solid adducts with the neutral ferrocene complexes. The stoichiometry of the CT complex varies widely and is, perhaps, dictated by factors such as the size and shape of the donor which affect packing in the solid state [36–38].

Formation of charge transfer complexes result in a tremendous increase in the β values of the mono as well as bisferrocenyl compounds (listed in Table 2(a–f)). The β of the acceptors were measured independently and are listed in Table 1. The observed β values cannot be obtained by a simple addition of the hyperpolarizability of the neutral compounds (**1–4**) to that of the acceptors in all cases. Although most of the acceptors are centrosymmetric, they have non-zero β values. This is because they form weak CT adducts with acetonitrile. In another solvent such as chloroform, which is a weaker donor, all the acceptors have near zero β values. Since the CT complexes have significant absorption at 532 nm (that is, at 2ω), the high β value can be explained by resonant contribution via a two photon mechanism. Dispersion free hyperpolarizability, β_0, was calculated using the two-state model considering only the absorption band close to the harmonic frequency. They are listed in Table 2(a–f). No simple correlation between β_0 and λ_{max} or β and λ_{max} can be found. Due to its approximate nature and complexities of specific solute–solvent interactions as pointed out by DeMartino et al. [39], it is not surprising that the simple two-state model fails to account for the nonresonant part of the hyperpolarizability of the CT complexes. It appears from the absorption spectra that the CT complexes have more than one absorption band in the vicinity of 532 nm and the contribution of the various excited states to the resonance enhancement of β is not easy to estimate. All of these states, some of them more than others could be responsible for the high second-order response of these compounds.

From the electrochemical data in acetonitrile (Table 1) we note that the oxidizing ability varies in the following order: CA < TCNQ < TCNE < DDQ < I_2.

While we do not find a simple correlation between β and $E_{1/2}$ of acceptor for the CT complexes, β_0 decreases as $E_{1/2}$ increases in the positive sense. This is consistent with the observation of Coe et al. that oxidation results in decreased β_0 values. Thus stronger acceptors should lead to smaller β. While large values of $\Delta E_{1/2}$ ($\Delta E_{1/2} = E_{1/2\ \text{acceptor}} - E_{1/2\ \text{ferrocenyl complex}}$) are expected to result in nearly ionic systems D^+A^-, small and negative values

of $\Delta E_{1/2}$ would lead to very little charge injection in the ground state. However, this situation would be reversed in the excited state. This might possibly explain why these complexes with small and negative values of $\Delta E_{1/2}$ have larger β than the neutral components. In the case of strong acceptors, the donor capacity of the ferrocene is significantly decreased resulting in reduced CT in the excited state.

5. Conclusion

In this paper, we have examined the quadratic polarizability of a series of Schiff base complexes containing one and two ferrocenyl units and their corresponding CT adducts. These organometallic compounds have large values of β, comparable to and in some cases, more than other known organometallic substances. The MLCT transitions dominate the second-order response of these molecules. The contribution of the ligand orbitals to the LUMO can be increased with suitable substitutions in the organic spacer that is attached to the cyclopentadienyl moiety of the ferrocene. This in turn, leads to large nonlinearities in the neutral ferrocenyl complexes. Also, most of these compounds absorb around 532 nm and consequently there is a significant contribution to β from two photon resonance enhancement. Formation of CT complexes enhances the second-order nonlinearity through two photon resonance enhancement. In fact, in the CT complexes, the nonresonant component of the first hyperpolarizability β_0 calculated through the two-state model, is not very large except in the case of CT complexes formed by chloranil (CA). These systems are similar to ruthenium bipyridyl complexes where oxidation lowers β_0. In ferrocenyl complexes, formation of CT adducts results in a adduct where electron density is transferred to an extended acceptor resulting in lower β_0. The results clearly encourage finding CT complexes with suitable redox couples for future NLO applications.

Acknowledgements

A.G.S. would like to thank the Department of Science and Technology, Government of India for funding part of this research. P.K.D. is grateful to the All India Council for Technical Education and the Council of Scientific and Industrial Research and also the Government of India, for generous funding. We thank Paresh Chandra Ray and K. Alagesan for helping us in the initial stages of this work.

References

[1] M.L.H. Green, S.R. Marder, M.E. Thompson, J.A. Bandy, D. Bloor, P.V. Kolinsky, R.J. Jones, Nature 330 (1987) 360.
[2] N.J. Long, Angew. Chem. Int. Ed. Engl. 34 (1995) 21.
[3] T. Verbiest, S. Houbrechts, M. Kauranen, K. Clays, A. Persoons, J. Mater. Chem. 7 (1997) 2175.
[4] D.R. Kanis, M.A. Ratner, T.J. Marks, J. Am. Chem. Soc. 114 (1992) 10338.
[5] S. Barlow, H.E. Bunting, C. Ringham, J.C. Green, G.U. Bublitz, S.G. Boxer, J.W. Perry, S.R. Marder, J. Am. Chem. Soc. 121 (1999) 3715.
[6] U. Hagenau, J. Heck, E. Hendrickx, A. Persoons, T. Schuld, H. Wong, Inorg. Chem. 35 (1996) 7863.
[7] K.N. Jayaprakash, P.C. Ray, I. Matsuoka, M.M. Bhadbhade, V.G. Puranik, P.K. Das, H. Nishihara, A. Sarkar, Organometallics 18 (1999) 3851.
[8] K. Alagesan, P.C. Ray, P.K. Das, A.G. Samuelson, Curr. Sci. 70 (1996) 9.
[9] K. Alagesan, Ph.D. Thesis, Indian Institute of Science, 1995.
[10] G.G.A. Balavoine, J.-C. Daran, G. Iftime, P.G. Lacriox, E. Manoury, J.A. Delaire, I. Maltey Fanton, K. Nakatani, S. Di Bella, Organometallics 18 (1999) 21.
[11] J.A. Campo, M. Cano, J.V. Heras, C. Lopez-Garabito, E. Pinilla, R. Torres, G. Rojo, F. Agullo-Lopez, J. Mater. Chem. 9 (1999) 899.
[12] E. Hendrickx, A. Persoons, S. Samson, G.R. Stephenson, J. Organomet. Chem. 542 (1997) 295.
[13] B.J. Coe, S. Houbrechts, I. Asselberghs, A. Persoons, Angew. Chem. Int. Ed. Engl. 38 (1999) 366.
[14] J.L. Oudar, J. Chem. Phys. 67 (1977) 446.
[15] I.R. Whittall, M.G. Humphrey, S. Houbrechts, A. Persoons, D.C.R. Hockless, Organometallics 15 (1996) 5738.
[16] K. Clays, A. Persoons, Phys. Rev. Lett. 66 (1991) 2980.
[17] K. Clays, A. Persoons, L. DeMaeyer, Adv. Chem. Phys. 85 (1994) 455.
[18] P.C. Ray, P.K. Das, J. Phys. Chem. 99 (1995) 14414.
[19] N.W. Song, T.-I. Kang, S.C. Jeoung, S.-J. Jeon, B.R. Cho, D. Kim, Chem. Phys. Lett. 261 (1996) 307.
[20] O.K. Song, J.N. Woodford, C.H. Wang, J. Phys. Chem. A 101 (1997) 3222.
[21] M. Stahelin, D.M. Burland, J.E. Rice, Chem. Phys. Lett. 191 (1992) 245.
[22] L. Meites, P. Zuman, CRC Handbook Series in Organic Electrochemistry, vol. 1, CRC, Boca Raton, FL, 1977.
[23] A.J. Bard, Encycl. Electrochem. Elements 1 (1973) 95.
[24] R. Bosque, C. Lopez, J. Sales, Inorg. Chim. Acta. 244 (1996) 141.
[25] L. Cun, P. Xin, Y. Xiao-Zeng, Synth. React. Inorg. Met. Org. Chem. 20 (1990) 1231.
[26] S.K. Pal, K. Alagesan, A.G. Samuelson, J. Pebler, J. Organomet. Chem. 575 (1999) 108.
[27] Y.S. Sohn, D.N. Hendrickson, H.B. Gray, J. Am. Chem. Soc. 93 (1971) 3603.
[28] A.T. Armstrong, A.T. Smith, E. Elder, S.P. McGlynn, J. Chem. Phys. 46 (1967) 4321.
[29] L.T. Cheng, W. Tam, D.F. Eaton, Organometallics 9 (1990) 2856.
[30] J.C. Calabrese, L.T. Cheng, J.C. Green, S.R. Marder, W. Tam, J. Am. Chem. Soc. 113 (1991) 7227.
[31] J.F. Nicoud, R.J. Twieg, in: D.S. Chemla, J. Zyss (Eds.), Nonlinear Optical Properties of Organic Molecules and Crystals, vol. 2, Academic Press, New York, 1987, pp. 255–267.
[32] A. Krishnan, P.K. Das, K.V. Katti, submitted for publication.

[33] A. Houlton, J.R. Miller, J. Silver, N. Jassim, M.J. Ahmet, T.L. Axon, D. Bloor, G.H. Cross, Inorg. Chim. Acta 205 (1993) 67.
[34] L.T. Cheng, W. Tam, S. Stevenson, G.R. Meredith, G. Rikken, S.R. Marder, J. Phys. Chem. 95 (1991) 10631.
[35] L.T. Cheng, W. Tam, S.R. Marder, A.E. Stiegman, G. Rikken, C.W. Spangler, J. Phys. Chem. 95 (1991) 10643.
[36] K.M. Chi, J.C. Calabrese, W.M. Reiff, J.S. Miller, Organometallics 10 (1991) 688.
[37] P.C. Junk, L.R. MacGillvray, M.T. May, K.D. Robinson, J.L. Atwood, Inorg. Chem. 34 (1995) 5395.
[38] H.H. Wei, I.S. Hwang, M.C. Cheng, Y. Wang, J. Organomet. Chem. 470 (1994) 161.
[39] R.N. DeMartino, E.W. Choe, G. Khanarian, D. Haas, T. Leslie, G. Nelson, J. Stamatoff, D. Stutz, C.C. Teng, H. Yoon, in: P.N. Prasad, D.R. Ulrich (Eds.), Nonlinear Optical and Electroactive Polymers, Plenum, New York, 1988, p. 169.